

000  
001  
002  
003 

# RAFT: REASONING-AWARE FINE-TUNING

  
004  
005  
006  
007  
008  
009010 **Anonymous authors**  
011  
012  
013  
014  
015  
016  
017  
018  
019  
020  
021  
022  
023  
024  
025  
026  
027  
028  
029  
030  
031  
032  
033  
034  
035  
036  
037  
038  
039  
040  
041  
042  
043  
044  
045  
046  
047  
048  
049  
050  
051  
052  
053010 Paper under double-blind review  
011  
012  
013  
014  
015  
016  
017  
018  
019  
020  
021  
022  
023  
024  
025  
026  
027  
028  
029  
030  
031  
032  
033  
034  
035  
036  
037  
038  
039  
040  
041  
042  
043  
044  
045  
046  
047  
048  
049  
050  
051  
052  
053

## ABSTRACT

Supervised fine-tuning (SFT) adapts large pretrained models to downstream tasks but often fails to learn reasoning-consistent mappings, especially under limited data. Chain-of-Thought (CoT) fine-tuning addresses this by training models to produce explicit reasoning traces, but at the cost of significantly increased inference latency and variable effectiveness across domains. We introduce *Reasoning-Aware Fine-Tuning (RAFT)*, a single-stage framework that distils reasoning signals during training without requiring reasoning generation at inference. RAFT leverages a reasoning-discriminative loss applied to positive and negative reasoning traces sampled from a teacher model, guiding the student to align its internal scoring with valid reasoning while preserving the efficiency of SFT. Our extensive experiments across visual reasoning, medical VQA, fine-grained recognition, and CommonsenseQA demonstrate that RAFT consistently outperforms SFT and CoT-FT baselines, while maintaining SFT-level inference efficiency. Beyond accuracy, we provide the systematic analysis of RAFT’s *scalability and robustness*: (i) performance improves monotonically with stronger teachers (3B-GPT-4.1), and (ii) RAFT remains effective even with noisy teacher supervision. Compared against preference-optimisation baselines, RAFT delivers complementary advantages by distilling reasoning rather than preferences.

## 1 INTRODUCTION

The advent of large pretrained models such as BERT (Devlin et al., 2019), GPT-2 (Radford et al., 2019), and GPT-3 (Brown et al., 2020) has revolutionised the field of artificial intelligence, offering unprecedented capabilities across a wide range of tasks. A key paradigm for leveraging their power for specific applications is Supervised Fine-Tuning (SFT) (Wei et al., 2021; Ouyang et al., 2022). SFT adapts these general-purpose models by further training them on smaller, task-specific datasets. This process updates the model’s parameters, enabling it to handle a broader range of tasks.

Although widely used, standard SFT is not without its limitations. Our empirical analysis in section 4.1 reveals that, when trained on limited non-reasoning data, SFT tends to learn *surface-level* correlations sufficient for producing correct answers, but does not capture the reasoning process underlying them, under limited supervision. For instance, as shown in Figure 1, an SFT model may produce the correct answer, but when asked to discriminate between correct and incorrect reasoning steps, it tends to prefer the incorrect one. This suggests that the model has not learned to ground its output in valid reasoning, but rather relies on spurious input-output patterns.

To address the limitations of SFT in capturing explicit input-output mapping, Chain-of-Thought (CoT) fine-tuning (Kim et al., 2023; Muennighoff et al., 2025; Ye et al., 2025) has gained traction. This approach mitigates the shortcomings of SFT by explicitly encouraging models to generate intermediate reasoning steps that lead to the final answer. By making the reasoning process explicit, CoT fine-tuning can significantly improve performance on tasks demanding complex, multi-step deduction (Muennighoff et al., 2025; Ye et al., 2025). However, this improvement comes at a cost. The generation of explicit reasoning inevitably increases the length of output sequences, thereby introducing a higher per-example inference latency as shown in Figure 5c. This can be a critical bottleneck for applications with strict online latency requirements. Furthermore, a recent study (Li et al., 2025) and our investigations reveal that CoT fine-tuning, while beneficial for complex tasks, could potentially diminish performance on tasks that do not *necessitate* such complex reasoning (e.g., visual recognition in Table 2), especially without sufficient high-quality reasoning data.

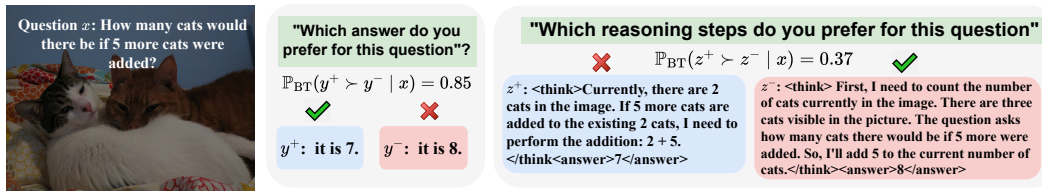


Figure 1: Illustration of the limitation of SFT in low-data regimes. Given a visual question, the SFT model trained on “prompt-answer” pairs correctly prefers the right answer with a high probability. However, the model shows a low preference for the correct reasoning. This suggests that such an SFT model can answer correctly without grasping the underlying valid reasoning process.

Therefore, we propose a novel fine-tuning pipeline **Reasoning-Aware Fine-Tuning (RAFT)**. The core of RAFT lies in its unique integration of reasoning supervision directly into the fine-tuning objective. This is achieved via a *reasoning-discriminative loss*, which explicitly guides the model to favour correct reasoning tokens over incorrect ones. The supervision for this discriminative process is derived from contrasting positive (correct) and negative (incorrect) reasoning examples, often sampled with the aid of a more capable teacher model. Crucially, this supervision is merely applied during training without necessitating the explicit generation of these reasoning tokens at inference time. Consequently, RAFT aims to preserve the computational efficiency characteristic of standard SFT while simultaneously enhancing the model’s ability to internally differentiate between valid and invalid reasoning. RAFT achieves significant accuracy improvements in visual reasoning and fine-grained recognition, demonstrating a highly effective and efficient approach to adapting models with an awareness of underlying reasoning discrimination.

The primary contributions of this work are: (i) Our analysis reveals that standard SFT, trained only on final answers, largely fails to distinguish between valid and flawed reasoning tokens. This highlights the critical need for RAFT’s explicit reasoning-aware supervision. (ii) *A general reasoning-distillation framework*: We propose RAFT, a single-stage fine-tuning method that introduces a reasoning-discriminative loss, enabling models to internalise reasoning signals without inference-time overhead. (iii) *Comprehensive empirical validation*: We show RAFT consistently improves performance across visual reasoning, fine-grained recognition, and text-only tasks, outperforming both SFT and CoT-FT under few-shot and low-resource conditions. (iv) *Scalability and robustness analysis*: We introduce a new metric, *Teacher CoT Accuracy*, to systematically measure the quality of reasoning supervision and demonstrate monotonic student performance improvements with stronger teachers (from 3B to GPT-4.1). We analyse the cost-performance trade-off, showing RAFT remains effective with reduced negative samples and maintains robustness under noisy supervision.

## 2 RELATED WORK

**Fine-tuning techniques.** Fine-tuning is the process of customising a large pre-trained model (Radford et al., 2019; Brown et al., 2020) to perform optimally on a specific task by further training it on a smaller, task-specific dataset. This process updates the model’s parameters to help it acquire new abilities, whereas in-context learning (Brown et al., 2020) leaves the model’s parameters unchanged. *SFT* (Wei et al., 2021; Ouyang et al., 2022; Liu et al., 2023)—where the model learns from example responses by maximising the likelihood. An earlier study, FLAN (Wei et al., 2021), shows that fine-tuning with a wide range of instruction-based datasets greatly improves zero-shot performance on tasks the model has not encountered before. *Direct Preference Optimisation (DPO)* (Rafailov et al., 2023)—where the model is shown both preferred and non-preferred responses to better capture subjective preferences; and *Reinforcement Fine-Tuning (RFT)* (Schulman et al., 2017; Jaech et al., 2024; Guo et al., 2025)—where the reinforcement learning technique is used to enhance the models’ reasoning capabilities in reasoning tasks such as solving mathematical problems (Luong et al., 2024; Shao et al., 2024b; Yang et al., 2024) and coding (Hui et al., 2024; Zhang et al., 2024b).

**SFT with reasoning data.** Recent research has emphasised the value of fine-tuning pre-trained models using datasets that include detailed reasoning steps (Muennighoff et al., 2025; Ye et al., 2025; Li et al., 2025). For example, Muennighoff et al. (2025) curated a high-quality dataset of 1000 question-reasoning pairs, carefully chosen for their challenge, diversity, and reasoning clarity. Fine-tuning the Qwen2.5 32B-Instruct model on this data led to performance gains of up to 27%

108 over 01-preview on competitive math questions. Similarly, LIMO (Ye et al., 2025) achieved 57.1%  
 109 accuracy on the demanding AIME benchmark by training on just 817 curated samples. However,  
 110 a recent study (Li et al., 2025) indicates that not all the tasks can benefit from fine-tuning with  
 111 reasoning data. Thus, the goal of our work is to explore whether we can leverage reasoning data to  
 112 improve task performance that seemingly does not require explicit reasoning outputs.

113 **Parameter-efficient fine-tuning (PEFT).** As state-of-the-art pre-trained models, such as GPT-4o  
 114 (Hurst et al., 2024), continue to grow in size and complexity, fully fine-tuning all their parameters  
 115 becomes increasingly resource-intensive and expensive. To address this challenge, recent research  
 116 has introduced PEFT strategies (Lester et al., 2021; Hu et al., 2022; Zhang et al., 2023a), which focus  
 117 on updating only a small subset of the model’s weights or incorporating lightweight modules such as  
 118 adapters (Zhang et al., 2023a), prompt tuning techniques (Lester et al., 2021), or low-rank adaptation  
 119 methods like LoRA (Hu et al., 2022). These approaches represent a significant advancement in the  
 120 field, as they enable practitioners to adapt large models to new tasks with substantially reduced  
 121 computational and memory requirements.

122 **Preference Optimisation.** Preference optimisation methods such as DPO (Rafailov et al., 2023),  
 123 ORPO (Hong et al., 2024), and GRPO (Shao et al., 2024b) have recently emerged as powerful  
 124 approaches for aligning large language models with human or synthetic preferences. These methods  
 125 train models to prefer desirable responses over undesirable ones by directly optimising preference  
 126 data. While highly effective for subjective alignment tasks (e.g., dialogue quality or safety), their  
 127 supervision signal focuses on end-level preferences rather than the intermediate reasoning process.  
 128 In contrast, RAFT complements these methods by explicitly distilling *reasoning signals*. Rather  
 129 than optimising for user preference, RAFT employs a reasoning-discriminative loss over positive  
 130 and negative reasoning traces, teaching the model to internally favour valid reasoning steps without  
 131 forcing reasoning generation at inference time. Thus, RAFT can be viewed as a reasoning-centric  
 132 counterpart to preference optimisation, offering orthogonal benefits in reasoning-intensive domains.  
 133 Detailed distinction with DPO can be found in section A.9.

134 **Scaling Laws of Chain-of-Thought.** Recent work has studied the scaling behaviour of Chain-of-  
 135 Thought (CoT) fine-tuning. Muennighoff et al. (2025) demonstrate that CoT benefits scale significantly  
 136 with model size and data quality, but improvements are concentrated in domains requiring  
 137 complex symbolic reasoning, such as mathematics and coding. Similarly, Sprague et al. (2024)  
 138 shows that the effectiveness of CoT is highly domain-dependent, with minimal or even negative  
 139 gains on recognition-heavy or low-data tasks. These findings highlight an important limitation:  
 140 while CoT excels in math/code settings, its efficiency and generalisation can degrade in broader  
 141 applications. RAFT addresses this gap by *leveraging reasoning supervision without inference-time*  
 142 *CoT generation*, allowing reasoning-aware improvements even in non-symbolic or low-resource do-  
 143 mains where CoT may struggle.

### 144 3 PRELIMINARIES

145 **Notation.** In this section, we introduce the mathematical notation in this paper. Let  $\mathcal{X}$  denote the  
 146 set of prompts and  $\mathcal{V}$  denote the set of vocabulary. The policy model<sup>1</sup>  $\pi_\theta$  parameterised by  $\theta$  outputs  
 147 a probability distribution  $\pi_\theta(\mathbf{y}|\mathbf{x})$ , where  $\mathbf{x} = [x_1, \dots, x_N] \in \mathcal{X}$  is the sequence of input tokens  
 148 and  $\mathbf{y} = [y_1, \dots, y_L] \in \mathcal{V}^L$  is the sequence of output tokens. Typically, the policy model  $\pi_\theta$  is  
 149 an auto-regressive model (Wang et al., 2024; Bai et al., 2025), meaning that it predicts the output  
 150 probability of the  $y_l$  given all tokens in  $\mathbf{x}$  and  $\mathbf{y}_{<l}$  as follows:

$$152 \quad \pi_\theta(\mathbf{y}|\mathbf{x}) := \prod_{l=1}^L \pi(y_l|\mathbf{x}, \mathbf{y}_{<l}), \quad (1)$$

153 where  $\mathbf{y}_{<l} := [y_1, \dots, y_{l-1}]$  and  $\mathbf{y}_{<1}$  is null.

154 **Problem setting.** The fundamental task addressed in this work is the adaptation of  $\pi_\theta$  for enhanced  
 155 performance on a downstream task given its training dataset  $\mathcal{D} = \{(\mathbf{x}_i, \mathbf{y}_i)\}_{i=1}^N$ , where  $\mathbf{x}_i \in \mathcal{X}$   
 156 represents input tokens and  $\mathbf{y}_i \in \mathcal{V}^*$  is the corresponding output tokens. Starting from a pre-trained  
 157 state, the model  $\pi_\theta$  is optimised to effectively map inputs  $\mathbf{x}$  characteristic of the downstream task to  
 158 their target outputs  $\mathbf{y}$ , typically by optimising an objective function derived from  $\mathcal{D}$ .

159 <sup>1</sup>The model we want to fine-tune.

162 **SFT.** SFT (Wei et al., 2021; Liu et al., 2023) is a standard approach to adapt  $\pi_\theta$  to a specific task  
 163 by directly maximising the likelihood of target outputs. Formally, given a dataset  $\mathcal{D}$ , the training  
 164 objective is to minimise the negative log-likelihood of the outputs conditioned on the input tokens:  
 165

$$166 \min_{\theta} \mathcal{J}_{\text{SFT}}(\theta) := -\mathbb{E}_{(\mathbf{x}, \mathbf{y}) \sim \mathcal{D}} [\log \pi_\theta(\mathbf{y} \mid \mathbf{x})]. \quad (2)$$

168 **CoT fine-tuning.** CoT fine-tuning (Kim et al., 2023; Muennighoff et al., 2025; Ye et al., 2025)  
 169 encourages  $\pi_\theta$  to produce the intermediate reasoning processes, improving performance on complex  
 170 reasoning tasks. Specifically, given a dataset  $\mathcal{D}_{\text{CoT}} = \{(\mathbf{x}_i, \mathbf{z}_i)\}_{i=1}^N$  where  $\mathbf{z}_i = (\mathbf{r}_i \oplus \mathbf{y}_i)$  denotes the  
 171 concatenation of the reasoning tokens  $\mathbf{r}$  and output answer tokens  $\mathbf{y}$ . CoT fine-tuning maximises the  
 172 likelihood of generating both the reasoning and the final answer tokens. Formally, the objective is  
 173

$$174 \min_{\theta} \mathcal{J}_{\text{CoT}}(\theta) := -\mathbb{E}_{(\mathbf{x}, \mathbf{z}) \sim \mathcal{D}_{\text{CoT}}} [\log \pi_\theta(\mathbf{z} \mid \mathbf{x})]. \quad (3)$$

175 By training the model to predict not only the final answer but also the reasoning tokens, this en-  
 176 ables  $\pi_\theta$  to have better performance on those complex tasks (Kim et al., 2023; Shao et al., 2024a).  
 177 However, producing both reasoning and answer typically increases the length of each generated se-  
 178 quence, which in turn raises *per-example inference time*. This might pose challenges for applications  
 179 with strict online inference latency requirements.  
 180

## 181 4 REASONING-AWARE FINE-TUNING

184 In this section, we conduct a preliminary step to show that standard SFT largely fails to discrimi-  
 185 nate between correct and incorrect reasoning, even though the model can output the correct answer  
 186 directly. Then we elaborate on the proposed method, RAFT.

### 187 4.1 ANALYSING THE ABILITY TO DISCRIMINATE REASONING DURING SFT

189 We investigate whether SFT (trained on  $(\mathbf{x}, \mathbf{y})$  pairs) en-  
 190 ables the model  $\pi_\theta$  to implicitly learn the underlying rea-  
 191 soning  $\mathbf{r}$  from a prompt  $\mathbf{x}$  to its corresponding answer  $\mathbf{y}$ .  
 192 Specifically, we aim to determine if models fine-tuned  
 193 with SFT develop an ability to recognise valid reason-  
 194 ing steps over incorrect ones. Understanding this is cru-  
 195 cial: if SFT models naturally learn to value correct rea-  
 196 soning, our task might merely involve amplifying this ex-  
 197 isting signal. However, if they do not, then a more direct  
 198 intervention to teach  $\pi_\theta$  for reasoning discrimination dur-  
 199 ing training is warranted. In this section, we empirically  
 200 investigate this research question:

201 *Does SFT of  $\pi_\theta$  on  $\mathcal{D}$  alone enable the model to implicitly learn to distinguish  
 202 valid reasoning pathways that map a prompt  $\mathbf{x}$  to its correct answer  $\mathbf{y}$ ?*

204 To assess whether SFT implicitly learn the reasoning discriminative capability, we must first address  
 205 a problem: standard SFT datasets  $\mathcal{D} = \{(\mathbf{x}_i, \mathbf{y}_i)\}_{i=1}^N$  lack explicit reasoning annotations. Thus, we  
 206 propose a *reasoning sampling protocol* to annotate the reasoning from a teacher model.  
 207

#### 208 4.1.1 REASONING SAMPLING PROTOCOL

209 **Reasoning sampling.** Here, we synthesise reasoning steps using a teacher model  $\pi^T$ . Even though  
 210  $\mathcal{D}$  lacks reasoning annotations, a teacher model (e.g., a larger pretrained model or human annotator)  
 211 can generate plausible reasoning  $\mathbf{r}_i^+$  that leads to  $\mathbf{y}_i$  and contrastive “distract” reasoning  $\mathbf{r}_i^-$  that  
 212 yields incorrect answers  $\mathbf{y}_i^- \neq \mathbf{y}_i$ . For each  $(\mathbf{x}_i, \mathbf{y}_i)$ , we generate contrastive reasoning tokens using  
 213 a teacher model  $\pi^T$ . For each prompt  $x_i$ , we sample  $k = 50$  completions from  $\pi^T$  with temperature  
 214  $T = 1$  and top- $p = 1$ :

$$215 \{ \mathbf{z}_i^{(1)}, \dots, \mathbf{z}_i^{(k)} \} \sim \pi^T(\cdot \mid \tilde{\mathbf{x}}_i), \quad (4)$$

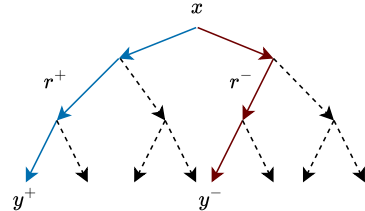
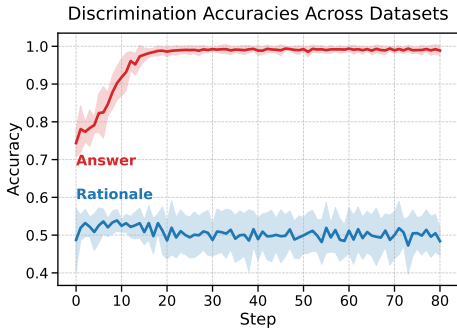


Figure 2: Illustrating the reasoning sam-  
 pling protocol.

216 where  $\tilde{\mathbf{x}}_i$  = “First reason step-by-step, then answer: ”  $\oplus \mathbf{x}_i$ . Among these completions, we select:  
 217

$$218 \quad \mathbf{z}_i^+ \sim \text{Uniform}\{\mathbf{z}_i^{(m)} : \mathbf{y}^{(m)} = \mathbf{y}_i\}, \quad \mathbf{z}_i^- \sim \text{Uniform}\{\mathbf{z}_i^{(m)} : \mathbf{y}^{(m)} \neq \mathbf{y}_i\}, \quad (5)$$

219 where  $\mathbf{z}_i^+ = \mathbf{r}_i^+ \oplus \mathbf{y}_i^+$ ,  $\mathbf{z}_i^- = \mathbf{r}_i^- \oplus \mathbf{y}_i^-$ . To further clarify our reasoning-trace construction proto-  
 220 col, we provide concrete worked examples in Appendix A.10. This ensures each training instance  
 221  $(\mathbf{x}_i, \mathbf{z}_i^+, \mathbf{z}_i^-)$  contains at least one valid positive and one valid negative reasoning path. If no valid  
 222 pair is found, we discard the instance for that epoch, preserving stability.  
 223



234 Figure 3: Discrimination acc.  
 235

236 partially correct but logically inconsistent reasoning. Results (see section 5) show RAFT remains stable  
 237 under such noise, demonstrating that its discriminative signal is resilient to imperfect supervision.  
 238

#### 241 4.1.2 REASONING DISCRIMINATION ACCURACY

243 To evaluate the ability of a model to distinguish between valid and invalid reasoning paths, we  
 244 define a unified metric: **Reasoning Discrimination Accuracy (RDA)**. Given a prompt  $x_i$  and a pair  
 245 of reasoning traces  $\mathbf{z}_i^+ = \mathbf{r}_i^+ \oplus \mathbf{y}_i^+$  (correct) and  $\mathbf{z}_i^- = \mathbf{r}_i^- \oplus \mathbf{y}_i^-$  (incorrect), we compute

$$246 \quad 247 \quad \text{RDA}(\pi) = \frac{1}{N} \sum_{i=1}^N \mathbb{I}\left[\tilde{\pi}(\mathbf{z}_i^+ | \mathbf{x}_i) > \tilde{\pi}(\mathbf{z}_i^- | \mathbf{x}_i)\right], \quad (6)$$

249 where  $\tilde{\pi}(z | x)$  denotes the length-normalised likelihood (Meng et al., 2024) of sequence  $z$  under  
 250 model  $\pi$ . A reasoning trace is considered positive only if its *final prediction matches the ground*  
 251 *truth*; Otherwise it is negative, regardless of fluency or surface probability. The likelihood is there-  
 252 fore not treated as an absolute proxy for reasoning quality, but only as a relative scoring signal: the  
 253 model is encouraged to rank verified-positive traces above verified-negative ones. This formulation  
 254 is consistent with preference-optimisation and reinforcement-style methods such as GRPO (Shao  
 255 et al., 2024b) and DPO (Rafailov et al., 2023), which also rely on relative likelihood comparisons  
 256 between desirable and undesirable responses. RDA can be applied to different models: (i) When  
 257  $\pi = \pi_T$  (teacher), RDA measures the reliability of teacher supervision (*Teacher CoT Accuracy*).  
 258 (ii) When  $\pi = \pi_\theta$  (student), RDA measures how well the student has internalized reasoning dis-  
 259 crimination (*Student Discrimination Accuracy*).  
 260

261 **Empirical results.** To examine what SFT learns, we directly evaluate the discriminative ability  
 262 of the model on its *training set* using the RDA metric (section 4.1.2). For each training instance,  
 263 we test whether the SFT model  $\pi_\theta$ <sup>2</sup> assigns higher likelihood to the ground-truth-verified reasoning  
 264 trace  $\mathbf{z}^+$  than to the incorrect reasoning trace  $\mathbf{z}^-$ . As shown in Figure 3, while SFT substantially im-  
 265 proves *answer discrimination*, its *reasoning discrimination* on the training set remains near chance.  
 266 This indicates that SFT effectively learns input–output mappings but fails to acquire the ability to  
 267 distinguish between  $\mathbf{r}^+$  and  $\mathbf{r}^-$ . The near-chance training-set discrimination performance demon-  
 268 strates the necessity of explicit supervision for reasoning discrimination, which motivates RAFT’s  
 269 reasoning-discriminative objective.

<sup>2</sup>The SFT model  $\pi_\theta$  is trained *only* on  $\mathcal{D}$  and does not observe  $(\mathbf{z}_i^+, \mathbf{z}_i^-)$  pairs or the teacher model  $\pi^T$  during its SFT phase.

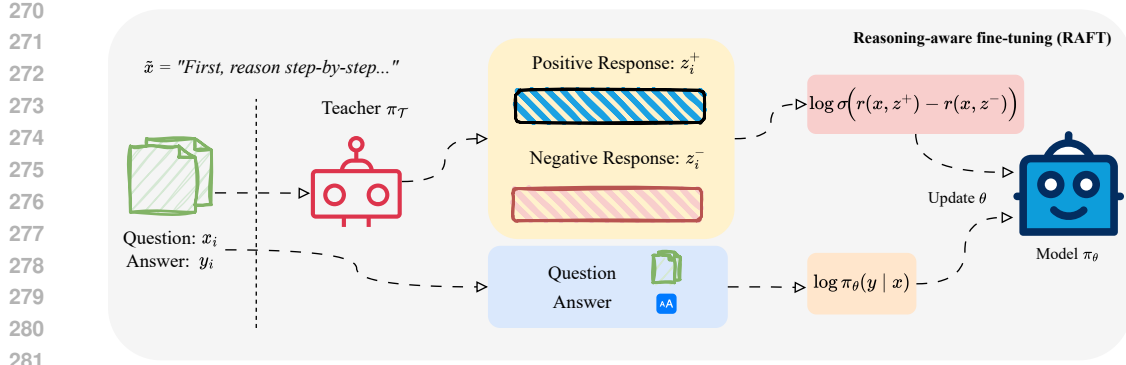


Figure 4: Overview of the RAFT pipeline. Given an input prompt, a refined prompt  $\tilde{\mathbf{x}}$  is appended to the input prompt, then passed to a teacher model to sample a pair of reasoning steps: a positive reasoning leading to the correct answer, and a negative reasoning leading to an incorrect one. The model is then fine-tuned to maximise the likelihood of the correct answer while learning to prefer the positive reasoning over the negative one using a reasoning discriminative objective.

#### 4.2 OBJECTIVE FOR REASONING-AWARE FINE-TUNING

A principled way to achieve this is to adopt the Bradley–Terry (BT) model (Bradley & Terry, 1952), a widely used probabilistic framework for modelling pairwise preferences. The BT model defines the probability that one candidate  $\mathbf{y}_1$  is preferred over another  $\mathbf{y}_2$  given an input  $\mathbf{x}$  as:

$$\mathbb{P}_{\text{BT}}(\mathbf{y}_1 \succ \mathbf{y}_2 | \mathbf{x}) = \sigma(r(\mathbf{y}_1) - r(\mathbf{y}_2)), \quad (7)$$

where  $r(\cdot)$  is a scalar function that represents the model’s internal preference, and  $\sigma(\cdot)$  is the sigmoid function. This formulation captures the intuition that the larger the margin between  $\mathbf{y}_1$  and  $\mathbf{y}_2$ , the more confident we are that  $\mathbf{y}_1$  is the preferred response. By incorporating this pairwise comparison into the training objective, we can directly supervise the model to assign higher likelihood to positive reasoning, thereby aligning its internal scoring function with the quality of reasoning paths, even when the model is trained only to produce final answers at inference time. We can come up with the following objective

$$-\mathbb{E}_{(\mathbf{x}, \mathbf{y}, \mathbf{z}^+, \mathbf{z}^-) \sim \mathcal{D}^{\text{RAFT}}} \left[ \underbrace{\log \pi_\theta(\mathbf{y} | \mathbf{x})}_{\text{SFT loss}} + \underbrace{\beta \log \sigma(r(\mathbf{x}, \mathbf{z}^+) - r(\mathbf{x}, \mathbf{z}^-))}_{\text{Reasoning discriminative loss}} \right], \quad (8)$$

where  $\beta$  is a weighting hyperparameter, and the reasoning discriminative loss term could be realised by the log of odds (Hong et al., 2024) as

$$\text{logit}(\mathbf{y} | \mathbf{x}) = \log \frac{\tilde{\pi}_\theta(\mathbf{y} | \mathbf{x})}{1 - \tilde{\pi}_\theta(\mathbf{y} | \mathbf{x})}, \quad (9)$$

where  $\frac{\tilde{\pi}_\theta(\mathbf{y} | \mathbf{x})}{1 - \tilde{\pi}_\theta(\mathbf{y} | \mathbf{x})} = k$  indicates that it is  $k$  times more likely for the model  $\tilde{\pi}_\theta$  to generate the output sequence  $\mathbf{y}$  than not generating it. Also,  $\sigma(r(\mathbf{x}, \mathbf{z}^+) - r(\mathbf{x}, \mathbf{z}^-))$  defines an odds ratio to indicate how likely it is for the model to generate  $\mathbf{z}^+$  than  $\mathbf{z}^-$ .

**Prompt perturbation.** To prevent the model from conditioning all three sequences  $\mathbf{y}$ ,  $\mathbf{z}^+$  and  $\mathbf{z}^-$  on the identical prompt  $\mathbf{x}$  in Equation 8, we slightly modify  $\mathbf{x}$  in the reasoning discriminative term as  $\tilde{\mathbf{x}}$ . We apply this prompt perturbation to disambiguate the SFT and reasoning discriminative loss, enabling the model to distinguish between imitation and comparison signals during training, while still supporting efficient, reasoning-free decoding at inference time. Thus, our final objective is

$$\mathcal{J}_{\text{RAFT}}(\theta) := -\mathbb{E}_{(\mathbf{x}, \mathbf{y}, \mathbf{z}^+, \mathbf{z}^-) \sim \mathcal{D}^{\text{RAFT}}} \left[ \log \pi_\theta(\mathbf{y} | \mathbf{x}) + \beta \log \sigma(\text{logit}(\mathbf{z}^+ | \tilde{\mathbf{x}}) - \text{logit}(\mathbf{z}^- | \tilde{\mathbf{x}})) \right], \quad (10)$$

**RAFT Outline.** The RAFT pipeline (Figure 4) is as follows: given a dataset  $\mathcal{D}$ , for each  $(\mathbf{x}_i, \mathbf{y}_i)$  we invoke a fixed teacher model  $\pi_T$  to sample  $(\mathbf{z}_i^+, \mathbf{z}_i^-)$  under a modified prompt  $\tilde{\mathbf{x}}_i$ . we fine-tune our policy model  $\pi_\theta$  by minimising the RAFT loss in Equation 10. Finally, at deployment

324  
325 Table 1: Performance comparison of different methods on Visual Reasoning and Visual Medical  
326 Reasoning benchmarks. Scores are reported as accuracy (%). The base model is Qwen2.5-VL-7B.  
327

Method	Visual Reasoning		Visual Medical Reasoning		Avg.
	CVQA	OmniMedVQA	PMC-VQA		
	51.81	65.00	48.00	54.94	
Qwen2.5-VL-7B (Bai et al., 2025)	51.81	65.00	48.00	54.94	
Qwen2.5-VL-72B (Bai et al., 2025)	71.08	67.38	55.60	64.68	
SFT (Wei et al., 2021)	58.46	81.50	49.80	63.25	
COT-FT (Kim et al., 2023)	58.00	83.13	46.60	62.58	
<b>RAFT (Ours)</b>	<b>64.47 <math>\pm</math> 0.04</b>	<b>87.63 <math>\pm</math> 0.10</b>	<b>53.53 <math>\pm</math> 0.07</b>	<b>68.54</b>	

334  
335 Table 2: Performance comparison of different methods on Fine-grained Visual Recognition (few-  
336 shot) benchmarks. Scores reported as Accuracy (%). The base model is Qwen2.5-VL-7B. RAFT  
337 shows mean  $\pm$  std over three runs (std on a second line).

Dataset	Zero-shot		1-shot			4-shot			8-shot		
	Qwen2.5-VL-7B	Qwen2.5-VL-72B	SFT	CoT-FT	RAFT	SFT	CoT-FT	RAFT	SFT	CoT-FT	RAFT
CUB	37.40	64.80	66.60	43.70	<b>71.50</b> $\pm 0.05$	79.70	60.70	<b>83.10</b> $\pm 0.04$	83.10	58.90	<b>84.80</b> $\pm 0.06$
S.Dogs	12.50	65.83	78.50	57.50	<b>80.30</b> $\pm 0.07$	81.83	60.50	<b>82.50</b> $\pm 0.05$	81.67	64.67	<b>83.83</b> $\pm 0.09$
F.Aircraft	42.75	62.00	70.57	46.00	<b>73.71</b> $\pm 0.06$	79.14	61.71	<b>81.14</b> $\pm 0.08$	81.43	65.43	<b>81.43</b> $\pm 0.07$
O.Pet	64.43	78.63	82.16	49.22	<b>84.32</b> $\pm 0.04$	81.62	72.97	<b>85.41</b> $\pm 0.05$	83.78	75.14	<b>84.86</b> $\pm 0.06$
S.Cars	35.77	75.71	73.47	37.96	<b>74.29</b> $\pm 0.05$	82.14	60.51	<b>83.98</b> $\pm 0.07$	85.41	70.20	<b>87.14</b> $\pm 0.06$
Avg.	38.57	69.40	74.26	46.87	<b>76.28</b>	80.89	63.28	<b>83.23</b>	83.08	66.87	<b>84.41</b>

348  
349 time, we condition only on  $\mathbf{x}_{\text{test}}$  so that the model produces the answer directly, omitting reasoning  
350 generation and thus preserving low-latency inference while retaining the benefits of reasoning-aware  
351 supervision. The overall algorithm can be found in the Appendix.

## 353 5 EXPERIMENTS

356 To empirically validate the effectiveness and efficiency of our proposed method RAFT, we con-  
357 ducted comprehensive experiments across diverse benchmark datasets.

359 **Implementation details.** Datasets and baselines can be found in Appendix A.1. During the training  
360 in all experiments, we use the Qwen2.5-VL-7B (Bai et al., 2025) vision-language model as  $\pi_\theta$ ,  
361 leveraging the PyTorch (Paszke, 2019) framework and the Hugging Face Transformers library (Wolf  
362 et al., 2019). Fine-tuning was performed on 8 NVIDIA H100 GPUs. We use the AdamW optimiser  
363 with a learning rate of 1e-4 and a cosine decay schedule (Loshchilov & Hutter, 2016) with a warm-  
364 up ratio of 0.05, using a global batch size of 32. Training proceeds for 400-1600 steps based on the  
365 size of the dataset. All the methods are fine-tuned with LoRA (Hu et al., 2022) with rank 4, alpha as  
366 8. For RAFT, the teacher model  $\pi^T$  used for sampling is Qwen2.5-VL-72B (Bai et al., 2025). The  
367 reasoning discriminative object weight  $\beta$  was set to 0.001, and we appended “First reason step-by-  
368 step, then answer” to the input prompt. Baselines are implemented following standard procedures;  
369 specifically, SFT and COT-FT use standard cross-entropy loss. Evaluation metrics follow common  
370 practice for each benchmark dataset.

371 **Visual reasoning results.** Table 1 summarises the performance comparison of RAFT against base-  
372 line methods on Visual Reasoning and Visual Medical Reasoning benchmarks, reporting accuracy  
373 (%). First, we can observe that integrating CoT with SFT leads to a discrepant effect, e.g., +1.6% on  
374 OmniMedVQA while -3.2% on PMC-VQA. This indicates that naively urging CoT output tokens  
375 does not always facilitate adaptation with downstream tasks. In contrast, RAFT demonstrates su-  
376 perior performance across all tasks, i.e., 65.08% on CVQA, 88.75% on OmniMedVQA, and 53.60%  
377 on PMC-VQA, providing its advantage in utilising reasoning. Second, compared with SFT, the  
378 proposed method attains notable performance gain, without sacrificing on inference efficiency (see  
379 analysis in Figure 5c). These results strongly validate the efficacy of the RAFT approach.

378 Table 3: Performance comparison of RAFT and DPO-based methods across reasoning and fine-  
 379 grained recognition benchmarks. Scores are reported as accuracy (%).  
 380

Method	CVQA	OmniMed	PMC	CUB	S.Dogs	F.Aircraft	Pet	S.Cars	Avg.
DPO (only)	45.08	60.88	50.60	47.40	67.50	52.00	75.68	47.65	55.85
DPO (2-stage)	58.62	86.38	50.20	67.90	79.17	69.43	80.00	73.06	70.60
SimPO (2-stage)	58.77	87.00	50.60	67.60	79.17	69.14	78.92	74.39	70.70
ORPO (2-stage)	59.23	86.88	51.00	68.40	77.00	68.29	80.54	73.57	70.61
RAFT ( <i>Ours</i> )	<b>65.08</b>	<b>88.75</b>	<b>53.60</b>	<b>71.50</b>	<b>80.17</b>	<b>73.71</b>	<b>83.24</b>	<b>74.29</b>	<b>73.79</b>

387 **Fine-grained visual recognition results.** To better validate the effectiveness of RAFT, we eval-  
 388 uated its performance on Fine-grained Visual Recognition tasks in a few-shot setting, with results  
 389 presented in Table 2. First, our method consistently yields improvement over all datasets with vary-  
 390 ing shots, which generally validates the effectiveness of the approach. Second, a noticeable phe-  
 391 nomenon is that CoT-FT leads to inferior performance on all scenarios. We conjecture that, under  
 392 limited data conditions, CoT-FT struggles to fully capture and internalise the logic expressed in CoT  
 393 reasoning. This suggests that enforcing CoT output is not always necessary or beneficial, particu-  
 394 larly in few-shot scenarios. However, as the amount of CoT-supervised data increases, we observe a  
 395 corresponding improvement in the performance of CoT fine-tuning. Nevertheless, our method can  
 396 still use this reasoning data to improve performance, which reflects the effectiveness of our method.  
 397

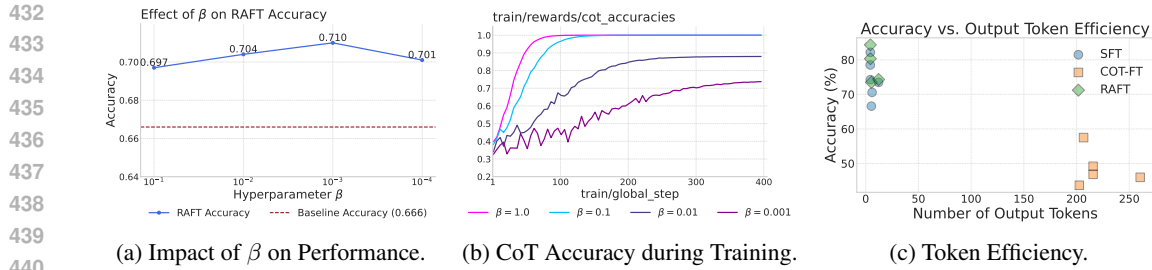
398 **Comparison with DPO-based Methods.** To ensure a fair comparison between RAFT and DPO-  
 399 style preference optimization, we carefully mirrored RAFT’s joint objective structure in our base-  
 400 lines. Specifically, for DPO we adopted a two-stage pipeline: (1) supervised fine-tuning (SFT) on  
 401 ground-truth labels to provide task supervision, followed by (2) preference optimisation over reason-  
 402 ing traces. This setup ensures that both RAFT and DPO variants are exposed to equivalent task-level  
 403 information and differ only in how preference signals are incorporated.

404 Empirical results are reported in Table 3. RAFT consistently outperforms both vanilla DPO and  
 405 stronger two-stage variants (SimPO, ORPO) across reasoning (CVQA, OmniMed, PMC-VQA) and  
 406 fine-grained recognition benchmarks (CUB, Stanford-Dogs, FGVC-Aircraft, Pet, Stanford-Cars),  
 407 achieving an average accuracy of **73.79%**, compared to  $\sim 70.6\text{--}70.7\%$  for the strongest DPO-based  
 408 baselines. These results validate that RAFT’s integrated supervision over both answers and reason-  
 409 ing traces yields stronger generalisation and higher task accuracy than DPO-style alternatives.  
 410

411 **Impact of Reasoning Discrimination Weight  $\beta$ .** We analyse the sensitivity of RAFT to the hy-  
 412 perparameter  $\beta$ , which balances the SFT loss with the reasoning-discriminative loss. The results,  
 413 presented in Figure 5, illustrate the dual impact of  $\beta$ : its effect on the final downstream task accuracy  
 414 and its influence on the model’s ability to learn discriminative reasoning. Figure 5a shows the final  
 415 accuracy achieved on a representative task across a range of  $\beta$  values, from  $10^{-1}$  down to  $10^{-4}$ .  
 416 We observe that an intermediate value, specifically  $\beta = 10^{-3}$ , yields the optimal performance. This  
 417 suggests that while reasoning supervision is beneficial, an excessively large  $\beta$  might overshadow the  
 418 primary task objective, or too small a  $\beta$  might not provide sufficient signal for learning robust rea-  
 419 soning. Concurrently, Figure 5b details the training dynamics of the model’s CoT accuracy, which  
 420 measures its proficiency in distinguishing correct from incorrect reasoning tokens. It is evident that  
 421 larger values of  $\beta$  (e.g.,  $\beta = 1.0$  and  $\beta = 0.1$ ) accelerate the learning of this discriminative capabil-  
 422 ity, leading to faster convergence and higher saturation levels in CoT accuracy. This confirms that  
 423 the reasoning discriminative loss is able to help distinguish the correct and incorrect reasoning steps.  
 424

425 **Token Efficiency.** One of the core advantages of RAFT lies in its ability to incorporate reason-  
 426 ing supervision during training while maintaining inference-time efficiency. Figure 5c compares  
 427 the average number of output tokens produced by SFT, CoT-FT, and RAFT across six fine-grained  
 428 visual recognition benchmarks. As shown, CoT-FT significantly increases the output length, often  
 429 requiring over 200 tokens per prediction due to its need to generate detailed reasoning. In con-  
 430 trast, both SFT and RAFT maintain concise outputs (typically under 15 tokens), making them more  
 431 suitable for latency-sensitive applications. Notably, RAFT matches or exceeds the performance of  
 432 CoT-FT while retaining the token efficiency of SFT, thereby offering a favourable trade-off between  
 433 reasoning ability and computational overhead.

434 **Influence of  $\pi^\tau$  Scale.** We conduct a systematic scaling study using Qwen2.5-VL teachers of  
 435 varying sizes (3B, 7B, 72B) and a GPT-4.1 teacher against a Zero-Shot baseline. As Figure 6 shows  
 436 that RAFT’s performance improves *monotonically* with stronger teachers across both reasoning and



432  
433  
434  
435  
436  
437  
438  
439  
440  
441  
442  
443  
444  
445  
446  
447  
448  
449  
450  
451  
452  
453  
454  
455  
456  
457  
458  
459  
460  
461  
462  
463  
464  
465  
466  
467  
468  
469  
470  
471  
472  
473  
474  
475  
476  
477  
478  
479  
480  
481  
482  
483  
484  
485

Figure 5: Detailed empirical analysis on fine-grained visual recognition tasks.

recognition benchmarks. This validates our theoretical motivation: the reasoning-discriminative loss transfers stronger reasoning signals when the teacher’s CoT accuracy is higher. Importantly, RAFT consistently improves over its SFT baseline even with small teachers (3B), demonstrating that RAFT is effective without requiring an extremely strong teacher.

**Sensitivity to Teacher Bias.** A natural concern is whether RAFT merely inherits the biases of the teacher model, rather than learning to prefer correct reasoning in its own right. In Figure 6: RAFT *remains effective even with weaker teachers* (baseline). This suggests that RAFT does not simply imitate teacher biases, but rather extracts useful contrastive reasoning signals across a range of teacher qualities. RAFT is explicitly designed to reduce sensitivity to individual teacher idiosyncrasies through two mechanisms: (1) **Pairwise, margin-based reasoning supervision.** RAFT does not directly imitate a single teacher’s reasoning trace. Instead, it compares positive and negative traces to construct a *relative preference signal*, which is more robust to noisy or biased reasoning than absolute imitation. (2) **SFT as the dominant learning signal.** RAFT combines this reasoning-discriminative objective with standard SFT on ground-truth answers. The SFT loss anchors training to correct answer prediction, while the reasoning-discriminative term acts as a regularizer that nudges the model toward internally consistent reasoning without overpowering the final-task supervision. Together, these design choices ensure that RAFT leverages teacher signals while mitigating the risk of copying spurious reasoning patterns.

**Additional Experiments and Analysis.** We include efficiency analysis in Appendix A.4, results on text-only benchmarks in Appendix A.2, impact of incorrect reasoning supervision in Appendix A.5, impact on the predicted answer likelihood in Appendix A.6, ablation on the reasoning discriminative loss in Appendix A.7, training dynamic Appendix A.8 and comparison with DPO in Appendix A.9.

## 6 CONCLUSION

In this work, we introduced RAFT, a novel single-stage method designed to leverage a reasoning-discriminative loss to guide models toward preferring correct over incorrect reasoning steps without requiring reasoning generation during inference. This allows RAFT to retain the computational efficiency of SFT while improving input-output alignment and generalisation, particularly in low-data and reasoning-intensive settings. Extensive experiments on visual reasoning and fine-grained recognition benchmarks demonstrate that RAFT consistently outperforms SFT and CoT-based fine-tuning approaches across multiple shot settings. We believe RAFT offers a general and scalable solution for improving MLLMs under limited supervision and opens up new directions for reasoning-aware alignment without incurring inference-time costs.

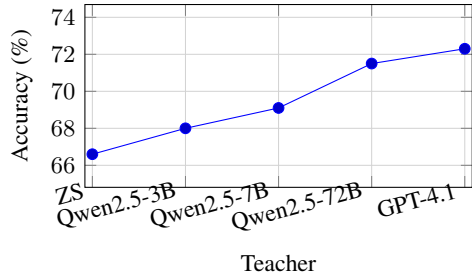


Figure 6: Teacher scaling: RAFT average accuracy improves monotonically with stronger teachers, validating robustness to teacher dependency.

486 REFERENCES  
487

488 Shuai Bai, Keqin Chen, Xuejing Liu, Jialin Wang, Wenbin Ge, Sibo Song, Kai Dang, Peng Wang,  
489 Shijie Wang, Jun Tang, et al. Qwen2. 5-vl technical report. *arXiv preprint arXiv:2502.13923*,  
490 2025.

491 Ralph Allan Bradley and Milton E Terry. Rank analysis of incomplete block designs: I. the method  
492 of paired comparisons. *Biometrika*, 39(3/4):324–345, 1952.

493

494 Tom Brown, Benjamin Mann, Nick Ryder, Melanie Subbiah, Jared D Kaplan, Prafulla Dhariwal,  
495 Arvind Neelakantan, Pranav Shyam, Girish Sastry, Amanda Askell, et al. Language models are  
496 few-shot learners. *Advances in neural information processing systems*, 33:1877–1901, 2020.

497

498 Jacob Devlin, Ming-Wei Chang, Kenton Lee, and Kristina Toutanova. Bert: Pre-training of deep  
499 bidirectional transformers for language understanding. In *Proceedings of the 2019 conference of  
500 the North American chapter of the association for computational linguistics: human language  
technologies, volume 1 (long and short papers)*, pp. 4171–4186, 2019.

501

502 Daya Guo, Dejian Yang, Haowei Zhang, Junxiao Song, Ruoyu Zhang, Runxin Xu, Qihao Zhu,  
503 Shirong Ma, Peiyi Wang, Xiao Bi, et al. Deepseek-r1: Incentivizing reasoning capability in llms  
504 via reinforcement learning. *arXiv preprint arXiv:2501.12948*, 2025.

505

506 Jiwoo Hong, Noah Lee, and James Thorne. Orpo: Monolithic preference optimization without  
507 reference model. *arXiv preprint arXiv:2403.07691*, 2024.

508

509 Edward J Hu, Yelong Shen, Phillip Wallis, Zeyuan Allen-Zhu, Yuanzhi Li, Shean Wang, Lu Wang,  
510 Weizhu Chen, et al. Lora: Low-rank adaptation of large language models. *ICLR*, 1(2):3, 2022.

511

512 Yutao Hu, Tianbin Li, Quanfeng Lu, Wenqi Shao, Junjun He, Yu Qiao, and Ping Luo. Omnimedvqa:  
513 A new large-scale comprehensive evaluation benchmark for medical lilm. In *Proceedings of the  
IEEE/CVF Conference on Computer Vision and Pattern Recognition*, pp. 22170–22183, 2024.

514

515 Binyuan Hui, Jian Yang, Zeyu Cui, Jiaxi Yang, Dayiheng Liu, Lei Zhang, Tianyu Liu, Jiajun Zhang,  
516 Bowen Yu, Keming Lu, et al. Qwen2. 5-coder technical report. *arXiv preprint arXiv:2409.12186*,  
517 2024.

518

519 Aaron Hurst, Adam Lerer, Adam P Goucher, Adam Perelman, Aditya Ramesh, Aidan Clark, AJ Os-  
520 trow, Akila Welihinda, Alan Hayes, Alec Radford, et al. Gpt-4o system card. *arXiv preprint  
arXiv:2410.21276*, 2024.

521

522 Aaron Jaech, Adam Kalai, Adam Lerer, Adam Richardson, Ahmed El-Kishky, Aiden Low, Alec  
523 Helyar, Aleksander Madry, Alex Beutel, Alex Carney, et al. Openai o1 system card. *arXiv  
preprint arXiv:2412.16720*, 2024.

524

525 Aditya Khosla, Nityananda Jayadevaprakash, Bangpeng Yao, and Fei-Fei Li. Novel dataset for fine-  
526 grained image categorization: Stanford dogs. In *Proc. CVPR workshop on fine-grained visual  
527 categorization (FGVC)*, number 1, 2011.

528

529 Seungone Kim, Se June Joo, Doyoung Kim, Joel Jang, Seonghyeon Ye, Jamin Shin, and Minjoon  
530 Seo. The cot collection: Improving zero-shot and few-shot learning of language models via  
531 chain-of-thought fine-tuning. *arXiv preprint arXiv:2305.14045*, 2023.

532

533 Jonathan Krause, Michael Stark, Jia Deng, and Li Fei-Fei. 3d object representations for fine-grained  
534 categorization. In *Proceedings of the IEEE international conference on computer vision work-  
shops*, pp. 554–561, 2013.

535

536 Brian Lester, Rami Al-Rfou, and Noah Constant. The power of scale for parameter-efficient prompt  
537 tuning. *arXiv preprint arXiv:2104.08691*, 2021.

538

539 Ming Li, Jike Zhong, Shitian Zhao, Yuxiang Lai, and Kaipeng Zhang. Think or not think: A study of  
540 explicit thinking in rule-based visual reinforcement fine-tuning. *arXiv preprint arXiv:2503.16188*,  
2025.

540 Haotian Liu, Chunyuan Li, Qingyang Wu, and Yong Jae Lee. Visual instruction tuning. *Advances*  
 541 *in neural information processing systems*, 36:34892–34916, 2023.  
 542

543 Ilya Loshchilov and Frank Hutter. Sgdr: Stochastic gradient descent with warm restarts. *arXiv*  
 544 *preprint arXiv:1608.03983*, 2016.

545 Trung Quoc Luong, Xinbo Zhang, Zhanming Jie, Peng Sun, Xiaoran Jin, and Hang Li. Reft: Rea-  
 546 soning with reinforced fine-tuning. *arXiv preprint arXiv:2401.08967*, 3, 2024.

547

548 Subhransu Maji, Esa Rahtu, Juho Kannala, Matthew Blaschko, and Andrea Vedaldi. Fine-grained  
 549 visual classification of aircraft. *arXiv preprint arXiv:1306.5151*, 2013.

550

551 Yu Meng, Mengzhou Xia, and Danqi Chen. Simpo: Simple preference optimization with a  
 552 reference-free reward. *Advances in Neural Information Processing Systems*, 37:124198–124235,  
 553 2024.

554

555 Niklas Muennighoff, Zitong Yang, Weijia Shi, Xiang Lisa Li, Li Fei-Fei, Hannaneh Hajishirzi, Luke  
 556 Zettlemoyer, Percy Liang, Emmanuel Candès, and Tatsunori Hashimoto. s1: Simple test-time  
 557 scaling. *arXiv preprint arXiv:2501.19393*, 2025.

558

559 Long Ouyang, Jeffrey Wu, Xu Jiang, Diogo Almeida, Carroll Wainwright, Pamela Mishkin, Chong  
 560 Zhang, Sandhini Agarwal, Katarina Slama, Alex Ray, et al. Training language models to fol-  
 561 low instructions with human feedback. *Advances in neural information processing systems*, 35:  
 562 27730–27744, 2022.

563

564 Omkar M Parkhi, Andrea Vedaldi, Andrew Zisserman, and CV Jawahar. Cats and dogs. In *2012*  
 565 *IEEE conference on computer vision and pattern recognition*, pp. 3498–3505. IEEE, 2012.

566

567 A Paszke. Pytorch: An imperative style, high-performance deep learning library. *arXiv preprint*  
 568 *arXiv:1912.01703*, 2019.

569

570 Alec Radford, Jeffrey Wu, Rewon Child, David Luan, Dario Amodei, Ilya Sutskever, et al. Language  
 571 models are unsupervised multitask learners. *OpenAI blog*, 1(8):9, 2019.

572

573 Rafael Rafailov, Archit Sharma, Eric Mitchell, Christopher D Manning, Stefano Ermon, and Chelsea  
 574 Finn. Direct preference optimization: Your language model is secretly a reward model. *Advances*  
 575 *in Neural Information Processing Systems*, 36:53728–53741, 2023.

576

577 John Schulman, Filip Wolski, Prafulla Dhariwal, Alec Radford, and Oleg Klimov. Proximal policy  
 578 optimization algorithms. *arXiv preprint arXiv:1707.06347*, 2017.

579

580 Hao Shao, Shengju Qian, Han Xiao, Guanglu Song, Zhuofan Zong, Letian Wang, Yu Liu, and Hong-  
 581 sheng Li. Visual cot: Advancing multi-modal language models with a comprehensive dataset and  
 582 benchmark for chain-of-thought reasoning. *Advances in Neural Information Processing Systems*,  
 583 37:8612–8642, 2024a.

584

585 Zhihong Shao, Peiyi Wang, Qihao Zhu, Runxin Xu, Junxiao Song, Xiao Bi, Haowei Zhang,  
 586 Mingchuan Zhang, YK Li, Y Wu, et al. Deepseekmath: Pushing the limits of mathematical  
 587 reasoning in open language models. *arXiv preprint arXiv:2402.03300*, 2024b.

588

589 Zayne Sprague, Fangcong Yin, Juan Diego Rodriguez, Dongwei Jiang, Manya Wadhwa, Prasann  
 590 Singhal, Xinyu Zhao, Xi Ye, Kyle Mahowald, and Greg Durrett. To cot or not to cot? chain-of-  
 591 thought helps mainly on math and symbolic reasoning. *arXiv preprint arXiv:2409.12183*, 2024.

592

593 Catherine Wah, Steve Branson, Peter Welinder, Pietro Perona, and Serge Belongie. The caltech-ucsd  
 594 birds-200-2011 dataset. 2011.

595

596 Peng Wang, Shuai Bai, Sinan Tan, Shijie Wang, Zhihao Fan, Jinze Bai, Keqin Chen, Xuejing Liu,  
 597 Jialin Wang, Wenbin Ge, et al. Qwen2-vl: Enhancing vision-language model’s perception of the  
 598 world at any resolution. *arXiv preprint arXiv:2409.12191*, 2024.

599

600 Jason Wei, Maarten Bosma, Vincent Y Zhao, Kelvin Guu, Adams Wei Yu, Brian Lester, Nan Du,  
 601 Andrew M Dai, and Quoc V Le. Finetuned language models are zero-shot learners. *arXiv preprint*  
 602 *arXiv:2109.01652*, 2021.

594 Jason Wei, Xuezhi Wang, Dale Schuurmans, Maarten Bosma, Fei Xia, Ed Chi, Quoc V Le, Denny  
 595 Zhou, et al. Chain-of-thought prompting elicits reasoning in large language models. *Advances in*  
 596 *neural information processing systems*, 35:24824–24837, 2022.

597

598 Thomas Wolf, Lysandre Debut, Victor Sanh, Julien Chaumond, Clement Delangue, Anthony Moi,  
 599 Pierrick Cistac, Tim Rault, Rémi Louf, Morgan Funtowicz, et al. Huggingface’s transformers:  
 600 State-of-the-art natural language processing. *arXiv preprint arXiv:1910.03771*, 2019.

601

602 An Yang, Beichen Zhang, Binyuan Hui, Bofei Gao, Bowen Yu, Chengpeng Li, Dayiheng Liu, Jian-  
 603 hong Tu, Jingren Zhou, Junyang Lin, et al. Qwen2. 5-math technical report: Toward mathematical  
 604 expert model via self-improvement. *arXiv preprint arXiv:2409.12122*, 2024.

605

606 Yixin Ye, Zhen Huang, Yang Xiao, Ethan Chern, Shijie Xia, and Pengfei Liu. Limo: Less is more  
 607 for reasoning. *arXiv preprint arXiv:2502.03387*, 2025.

608

609 Letian Zhang, Xiaotong Zhai, Zhongkai Zhao, Yongshuo Zong, Xin Wen, and Bingchen Zhao. What  
 610 if the tv was off? examining counterfactual reasoning abilities of multi-modal language models.  
 In *Proceedings of the IEEE/CVF Conference on Computer Vision and Pattern Recognition*, pp.  
 21853–21862, 2024a.

611

612 Renrui Zhang, Jiaming Han, Chris Liu, Peng Gao, Aojun Zhou, Xiangfei Hu, Shilin Yan, Pan Lu,  
 613 Hongsheng Li, and Yu Qiao. Llama-adapter: Efficient fine-tuning of language models with zero-  
 614 init attention. *arXiv preprint arXiv:2303.16199*, 2023a.

615

616 Xiaoman Zhang, Chaoyi Wu, Ziheng Zhao, Weixiong Lin, Ya Zhang, Yanfeng Wang, and Weidi  
 617 Xie. Pmc-vqa: Visual instruction tuning for medical visual question answering. *arXiv preprint*  
*arXiv:2305.10415*, 2023b.

618

619 Yuxiang Zhang, Shangxi Wu, Yuqi Yang, Jiangming Shu, Jinlin Xiao, Chao Kong, and Jitao Sang.  
 620 o1-coder: an o1 replication for coding. *arXiv preprint arXiv:2412.00154*, 2024b.

621

622

623

624

625

626

627

628

629

630

631

632

633

634

635

636

637

638

639

640

641

642

643

644

645

646

647

648 **A APPENDIX**649 **A.1 DATASETS AND BASELINES.**

650 To comprehensively evaluate our method, we utilise a range of benchmark datasets spanning different visual tasks. For general visual reasoning, we employ the CVQA (Zhang et al., 2024a) dataset. 651 To assess performance in the specialised domain of visual medical reasoning, we include OmniMed- 652 VQA (Hu et al., 2024) and PMC-VQA (Zhang et al., 2023b). For this task, we used 128 samples for 653 training and the remaining samples as the test set. Meanwhile, we also test the model’s capabilities 654 on fine-grained visual recognition in a challenging 1-shot, 4-shot, and 8-shot setting using five standard 655 datasets: CUB (Caltech-UCSD Birds-200-2011 (Wah et al., 2011)), Stanford-Dogs (S.Dogs 656 (Khosla et al., 2011)), Stanford-Cars (S.Cars (Krause et al., 2013)), FGVC-Aircraft (F.Aircraft (Maji 657 et al., 2013)), and Oxford-IIIT Pet (O.Pet (Parkhi et al., 2012)). We split the training and test sets 658 according to the number of shots.

659 To evaluate the performance of RAFT, we compare it against baselines representing different fine- 660 tuning and evaluation strategies. These include: Zero-Shot (ZS) evaluation to assess the pre-trained 661 model’s capability without any fine-tuning; standard Supervised Fine-Tuning (SFT) on the target 662 answers; Chain-of-Thought Fine-Tuning (CoT-FT) (Kim et al., 2023; Muennighoff et al., 2025; Ye 663 et al., 2025) where the model is trained on concatenated reasoning and answer sequences. We also 664 compare our method DPO-like methods (DPO (Rafailov et al., 2023), SimPO (Meng et al., 2024), 665 ORPO (Hong et al., 2024)).

666 **A.2 RESULTS ON TEXT-ONLY BENCHMARKS**

667 To further validate the generality of RAFT beyond multimodal reasoning, we evaluate on text-only 668 benchmarks covering commonsense reasoning and sentiment classification. Specifically, we consider 669 **CommonsenseQA (CSQA)** and **IMDb sentiment classification**. The base model is Qwen2.5- 670 7B (text-only variant).

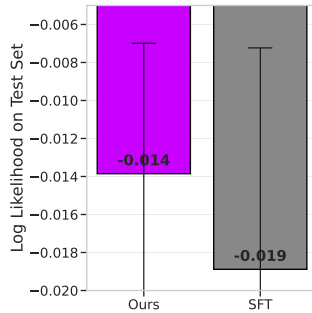
671 Table 4: Performance comparison on text-only benchmarks. Scores are reported as accuracy (%).  
672 The base model is Qwen2.5-7B.

Method	Text-only Benchmarks	
	CSQA	IMDb
SFT (Wei et al., 2021)	73.2	91.5
CoT-FT (Wei et al., 2022)	74.1	91.0
DPO (Rafailov et al., 2023)	74.6	91.7
<b>RAFT (Ours)</b>	<b>76.8</b>	<b>92.4</b>

673 **Discussion.** The results in Table 4 demonstrate that RAFT consistently outperforms both SFT 674 and CoT-FT on text-only tasks. On CommonsenseQA, RAFT achieves a  $\sim 2.7\%$  absolute improvement 675 over SFT, highlighting its ability to distill reasoning signals even in purely textual settings. 676 On IMDb, RAFT yields a modest but consistent gain, showing that the reasoning-discriminative signal remains 677 beneficial for classification-style tasks. These results confirm that RAFT’s benefits are not confined to multimodal 678 reasoning, but extend to general natural language understanding.

679 **A.3 ANALYSIS OF TEST SET LOG LIKELIHOOD.**

680 Figure 7 illustrates the average log likelihood assigned to 681 correct predictions on the test set, comparing the RAFT 682 against the standard SFT baseline. The bar chart clearly 683 indicates that the RAFT achieves an average log likelihood 684 of approximately -0.014, whereas the SFT model 685 attains a lower average log likelihood of approximately 686 -0.019. A higher log likelihood (i.e., a less negative value) 687 signifies that the model assigns greater 688



689 Figure 7: Log likelihood on test set.

702 likelihood to the ground-truth correct answers. This outcome suggests that RAFT develops a better  
 703 internal model for generating correct outputs, leading to improved confidence and accuracy on  
 704 unseen test data compared to SFT.

#### 706 A.4 EFFICIENCY ANALYSIS

708 To better understand the trade-offs of RAFT, we compare training and inference efficiency against  
 709 SFT and CoT-FT on the **CUB-200-2011** dataset, using identical hardware (A100 80GB GPU) and  
 710 training configurations. Table 5 reports the following metrics:

- 712 • **Annotation Time:** Average time to prepare one training example (reasoning traces re-  
 713 quired only for RAFT).
- 714 • **Training Time per Epoch:** Average time to complete one training epoch.
- 715 • **Training Throughput:** Number of training samples processed per second.
- 716 • **Average Output Length:** Average number of tokens generated during inference.
- 717 • **Inference Time:** Total time to process 1000 test samples.

719  
 720 Table 5: Comparison of training and inference efficiency across methods. RAFT introduces addi-  
 721 tional training overhead but retains SFT-level inference efficiency.

722 Method	Annotation Time	Training Time / Epoch	723 Train Samples / Sec	Avg. Output Length	Inference Time
724 SFT	0s	1m 10s	725 2.021	12 tokens	17s
CoT-FT	0s	1m 15s	1.869	210 tokens	1m 25s
RAFT ( <i>Ours</i> )	~0.065s	4m 12s	0.523	13 tokens	17s

726 **Observations.** We draw three key conclusions from Table 5:

727

- 729 1. **Training cost.** RAFT introduces overhead during training, with epoch time  $\sim 3\text{--}4 \times$  longer  
 730 than SFT and throughput reduced by more than half. This is primarily due to the reasoning-  
 731 discriminative loss, which requires sampling and contrasting positive vs. negative reasoning  
 732 traces.
- 733 2. **Annotation cost.** Preparing RAFT training instances adds a one-time annotation cost  
 734 ( $\sim 0.065\text{s}$  per sample), which is amortized across epochs.
- 735 3. **Inference efficiency.** Despite higher training cost, RAFT produces short outputs compa-  
 736 rable to SFT (12–13 tokens), in stark contrast to CoT-FT which generates  $\sim 210$  tokens.  
 737 Consequently, RAFT matches SFT’s inference speed (17s for 1000 samples) while being  
 738 significantly faster than CoT-FT.

739 **Takeaway.** RAFT trades off higher *training* cost for improved reasoning-aware alignment, while  
 740 retaining SFT-like *inference* efficiency. This makes RAFT particularly suitable for deployment sce-  
 741 narios where inference latency is critical but training resources are more flexible (e.g., server-side  
 742 fine-tuning, low-shot domain adaptation).

#### 744 A.5 IMPACT OF INCORRECT REASONING SUPERVISION

746 To further underscore the critical importance of learning from *valid* reasoning pathways during train-  
 747 ing, we conducted an ablation study. In this experiment, instead of guiding the model with correct  
 748 rationales as in RAFT, we explicitly prompted and trained the model to generate and internalise  
 749 incorrect or flawed reasoning steps leading to (potentially) correct or incorrect final answers. The  
 750 objective was to determine if the mere presence of a reasoning-like structure, even if faulty, could  
 751 offer any benefit, or conversely, how detrimental learning incorrect reasoning would be. The per-  
 752 formance impact was significant, as summarised below:

753 Training Condition	754 Accuracy
754 Valid Reasoning Supervision	65%
755 Incorrect Reasoning Supervision	49%

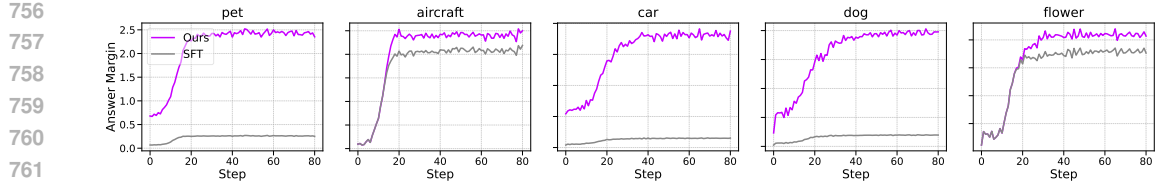


Figure 8: Comparison of the answer margins by RAFT (Ours) and SFT across training steps for various fine-grained visual recognition datasets: pet, aircraft, car, dog, and flower. This illustrates that reasoning and discrimination ability can encourage models to generate more confident answers.

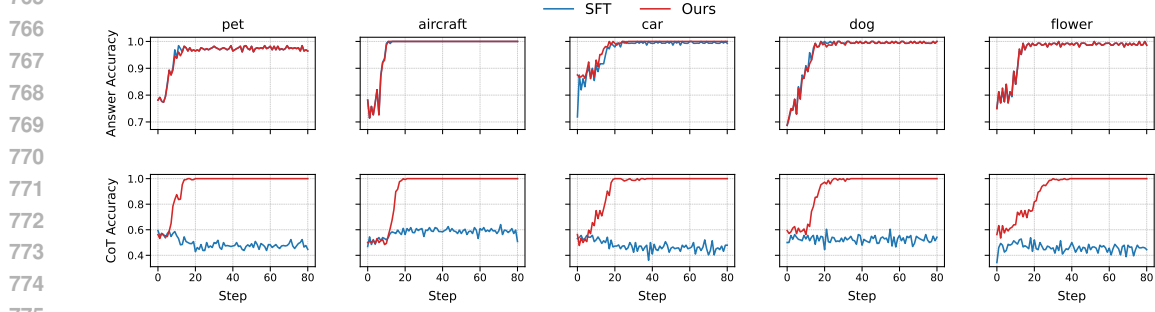


Figure 9: Training dynamics comparing RAFT (Ours) and SFT on fine-grained visual recognition datasets. The top row displays Answer Accuracy. The bottom row in the plot illustrates the model’s ability to discriminate between positive and negative reasoning steps.

As evidenced by the table, compelling the model to learn from explicitly incorrect reasoning pathways led to a substantial degradation in task performance, with accuracy dropping from 0.65 to 0.49. This stark decrease highlights that the model does not simply ignore faulty reasoning but actively learns detrimental patterns, thereby corrupting its ability to arrive at correct solutions. This finding strongly supports our hypothesis that the positive impact of RAFT stems directly from the quality and correctness of the reasoning signals it integrates, and that indiscriminate or erroneous reasoning supervision is actively harmful.

#### A.6 IMPACT ON THE PREDICTED ANSWER LIKELIHOOD

Figure 8 provides a comparative analysis of the answer margins achieved by RAFT versus standard SFT across various fine-grained visual recognition datasets, plotted over training steps. The "Answer Margin" on the y-axis represents the model’s confidence in its prediction, the difference in log-probabilities between the chosen answer and the next best alternative. Consistently, across all five datasets, the RAFT model (labelled "Ours") exhibits a notably higher answer margin compared to SFT throughout the training process. This observation suggests that RAFT’s enhanced reasoning discrimination capability, trained by distinguishing between positive and negative reasoning tokens, encourages the model to generate more confident and decisive correct answers.

#### A.7 ABLATION ON THE REASONING DISCRIMINATIVE LOSS

As demonstrated in Table 6, incorporating the reasoning discriminative loss leads to a consistent performance improvement. The loss contains a term with a negative gradient that reduces the model’s odds for the incorrect reasoning  $z^-$ . To assess its necessity, we conduct an ablation study where we removed this term. On the CUB fine-grained classification dataset, this leads to a performance drop of 2.9%. Furthermore, we investigate whether the gradient term for increasing the odds of the correct reasoning  $z^+$  is equally crucial. Omitting this term resulted in a dramatic performance drop of 19%, underscoring its critical role in enabling the model to prefer high-quality reasoning. These results affirm that both positive and negative preference gradients are essential for RAFT’s reasoning discrimination capabilities.

Table 6: Ablation of loss terms w.r.t relative accuracy.

Method	Acc. (%)
RAFT	71.50
w/o $z^-$	-2.90
w/o $z^+$	-19.00
w/o $z^+$ & $z^-$ (SFT)	-4.90

810 A.8 TRAINING DYNAMICS  
811

812 Figure 9 compares the training dynamics of RAFT and standard SFT across fine-grained visual  
813 recognition datasets. The top row illustrates *answer accuracy*, where RAFT (orange) consistently  
814 outperforms SFT (blue), achieving higher final accuracy across all datasets. Notably, the gap widens  
815 as training progresses, suggesting RAFT’s reasoning-aware training enables more effective learning.  
816 The bottom row, labelled *CoT Accuracy*, measures the model’s ability to discriminate between cor-  
817 rect and incorrect reasoning steps by evaluating the margin between log-probabilities of positive  
818 versus negative reasoning tokens. RAFT exhibits a steady improvement in this metric, reflecting its  
819 enhanced internal reasoning discrimination. In contrast, SFT stagnates near chance levels (50%),  
820 corroborating the hypothesis that SFT fails to internalise reasoning signals without explicit supervi-  
821 sion. These results validate RAFT’s dual benefit: improving answer accuracy while fostering robust  
822 reasoning discrimination, all without incurring the inference latency of explicit reasoning genera-  
823 tion.

824 A.9 COMPARISON BETWEEN RAFT AND DPO  
825

826 Direct Preference Optimization (DPO) (Rafailov et al., 2023) is a preference-learning framework  
827 that optimizes a model to prefer responses  $y^+$  over  $y^-$  given the same prompt  $x$ , using a KL-  
828 regularised objective. Formally, DPO maximises:

$$829 \mathcal{L}_{\text{DPO}}(\theta) = \mathbb{E}_{(x, y^+, y^-) \sim \mathcal{D}} \left[ \log \sigma \left( \beta \cdot \left( \log \frac{\pi_\theta(y^+|x)}{\pi_{\text{ref}}(y^+|x)} - \log \frac{\pi_\theta(y^-|x)}{\pi_{\text{ref}}(y^-|x)} \right) \right) \right], \quad (11)$$

830 where  $\pi_\theta$  is the student model,  $\pi_{\text{ref}}$  is a frozen reference model, and  $\beta$  controls the sharpness of the  
831 preference.

832 In contrast, RAFT introduces a *reasoning-discriminative* term over **reasoning traces**, not final out-  
833 puts. Given a prompt  $x$ , ground-truth answer  $y$ , and teacher-sampled reasoning traces  $z^+ = r^+ \oplus y$   
834 and  $z^- = r^- \oplus y^-$ , RAFT minimizes:

$$835 \mathcal{L}_{\text{RAFT}}(\theta) = -\mathbb{E}_{(x, y, z^+, z^-) \sim \mathcal{D}_{\text{RAFT}}} \left[ \log \pi_\theta(y | x) + \beta \cdot \log \sigma(\text{logit}_\theta(z^+ | \tilde{x}) - \text{logit}_\theta(z^- | \tilde{x})) \right], \quad (12)$$

836 where  $\tilde{x}$  is a perturbed prompt used to decouple the SFT and reasoning objectives, and  $\text{logit}_\theta(\cdot)$   
837 denotes the normalized log-likelihood.

841  
842 **Key Distinctions:**

- 843 • **Supervision signal:** DPO relies on *end-level preferences* over answers, while RAFT relies  
844 on *reasoning-level supervision* (contrasting valid vs. invalid reasoning traces).
- 845 • **Reference model:** DPO requires a frozen reference model  $\pi_{\text{ref}}$  to anchor preferences.  
846 RAFT does not require a reference model, instead depending on a teacher model  $\pi_T$  to  
847 generate contrastive reasoning.
- 848 • **Inference behavior:** DPO affects the model’s distribution over final answers. RAFT pre-  
849 serves standard SFT decoding at inference and introduces reasoning supervision *only dur-  
850 ing training*, hence maintaining SFT-level inference efficiency.
- 851 • **Objective structure:** DPO is a KL-regularised preference optimisation objective; RAFT  
852 is a hybrid objective: SFT loss on final answers + reasoning-discriminative loss.

855 A.10 ILLUSTRATIVE EXAMPLES OF REASONING DATA GENERATION  
856

857 These examples demonstrate how both *positive* and *negative* reasoning traces are systematically  
858 derived from teacher model completions.

859  
860 **Prompting the Teacher for Reasoning Traces.** To obtain reasoning–answer pairs from the  
861 teacher model  $\pi^T$ , we use a structured prompt that explicitly separates the reasoning process from  
862 the final answer. The teacher is instructed to produce its chain of thought within special tags  
863 `<think> ... </think>` and the final prediction within `<answer> ... </answer>`. An exam-  
864 ple of the prompting template is shown below:

864 You are solving a visual question answering problem.  
 865

866 **\*\*Action: Thinking\*\***  
 867 - Outline the step-by-step thinking process to solve the problem.  
 868 - Use the `<think>` tags to detail your process.  
 869

870 **\*\*Action: Answer\*\***  
 871 - Output your final answer within the `<answer>` tag with  
 872 just one word or one option.  
 873

874 Example:  
 875 `<answer>5</answer>`  
 876

877 Q: {question}  
 878 A:  
 879

Given this query format, each sampled completion naturally decomposes into two parts: (1) a reasoning trace  $r_i$  extracted from the `<think>` block, and (2) a final answer  $y_i$  extracted from the `<answer>` block. We then categorize the trace as a **positive sample**  $z_i^+ = r_i^+ \oplus y_i^+$  if  $y_i^+ = y_i$  matches the ground-truth label, or as a **negative sample**  $z_i^- = r_i^- \oplus y_i^-$  if  $y_i^- \neq y_i$ .  
 880 This explicit prompting strategy guarantees a clean separation between reasoning and answers, enabling us to systematically construct contrastive reasoning pairs. Moreover, it ensures reproducibility: the same template is applied consistently across all benchmarks.  
 881

882 **Extracting Reasoning Traces and Answers.** Given a prompt  $x_i$ , we query the teacher model  $\pi^T$  using a structured template that explicitly separates reasoning from the final prediction. The teacher is instructed to output their reasoning process inside `<think>` tags, and the final answer inside `<answer>` tags. This makes it straightforward to parse the output into a reasoning trace  $r_i$  and a candidate answer  $y_i$ .  
 883

884 For example, the teacher may produce:  
 885

886 `<think>`  
 887 The bird has bright yellow underparts and a thin curved beak,  
 888 traits characteristic of a yellow warbler.  
 889 `</think>`  
 890 `<answer>Yellow Warbler</answer>`  
 891

892 From this output, we extract:  
 893 
$$z_i^+ = r_i^+ \oplus y_i^+ \quad \text{if } y_i^+ = y_i,$$
  
 894 where  $y_i$  is the ground-truth label. If instead the final answer  $y_i^-$  does not match  $y_i$ , the corresponding reasoning trace  $z_i^- = r_i^- \oplus y_i^-$  is treated as a negative example, provided that the reasoning remains semantically plausible.  
 895

900 **Implementation detail.** We use a lightweight regular expression to extract the answer token from the teacher's output:  
 901

```
902 match = re.search(r'<answer>(.*)</answer>', output, re.DOTALL)
```

903 This guarantees consistent answer parsing across all datasets. Reasoning traces are preserved from the `<think>` block, while only the final token inside `<answer>` is compared against the ground truth.  
 904

912 In the first example (fine-grained bird classification), the teacher produces multiple reasoning-answer completions for the input image prompt “What is the type of this bird?”. From these, we select a **positive trace** that ends with the correct answer (*Yellow Warbler*) and whose intermediate reasoning is logically consistent (e.g., identifying yellow underparts and a thin curved beak). We then select a **negative trace** that ends with an incorrect label (*Song Thrush*), but whose reasoning remains plausible (e.g., citing mottled brown plumage and a stout beak). This ensures that the negative is not trivial noise but a semantically coherent alternative.  
 913

918

919

920

921

922

923

924

925

926

927

928

929

930

931

932

933

934

935

936

937

938

939

940

941

In the second example (CommonsenseQA), the prompt “Where would you expect to find a pizzeria while shopping?” with multiple-choice answers is used. The **positive trace** correctly reasons that shopping malls contain food courts with restaurants, leading to the answer *food court*. The **negative trace**, in contrast, incorrectly concludes that because Chicago is famous for deep-dish pizza, the answer should be *chicago*. Here again, the negative remains contextually relevant but incorrect, providing a meaningful contrastive supervision signal.

942

943

944

945

946

947

948

949

950

951

952

953

**Question:** Where would you expect to find a pizzeria while shopping?

A: chicago B: street C: little italy D: food court E: capital cities

**Positive CoT (chosen):** *When people go shopping, especially in malls or shopping centers, there are usually food courts where a variety of restaurants, including pizzerias, are located. Therefore, the answer is food court.*

**Negative CoT (rejected):** *Chicago is famous for deep-dish pizza, so one might expect to find a pizzeria there. Therefore, the answer is chicago.*

These examples illustrate how RAFT leverages contrastive reasoning supervision: for each instance, we guarantee at least one valid positive and one valid negative reasoning trace, ensuring stability during training. By pairing logically sound but incorrect reasoning with correct reasoning, RAFT teaches the student model to discriminate between valid and invalid reasoning paths without requiring explicit reasoning generation at inference time.

954

955

956

957

958

959

960

961

962

963

964

965

966

967

968

969

970

971



- Prompt with image ( $\mathbf{x}_i$ ): “What is the type of this bird?”
- Positive Response ( $\mathbf{r}_i^+ \oplus \mathbf{y}_i^+$ ): “It has bright yellow underparts and a thin, slightly curved beak—features characteristic of a **yellow warbler**.”
- Positive Answer ( $\mathbf{y}_i^+$ ): “Yellow Warbler”
- Negative Response ( $\mathbf{r}_i^- \oplus \mathbf{y}_i^-$ ): “It has mottled brown plumage and a stout beak—traits seen in many thrush species. So it is a **Song Thrush**.”
- Negative Answer ( $\mathbf{y}_i^-$ ): “Song Thrush”

972    **A.11 REPRODUCIBILITY STATEMENT**  
973

974    Code, training scripts, and evaluation utilities will be publicly released upon publication.  
975

976    **A.12 AI USAGE CLARIFICATION**  
977

978    Large Language Models were employed solely to enhance grammar and readability. All aspects of  
979    research design, analysis, and interpretation were conducted by the authors.  
980  
981  
982  
983  
984  
985  
986  
987  
988  
989  
990  
991  
992  
993  
994  
995  
996  
997  
998  
999  
1000  
1001  
1002  
1003  
1004  
1005  
1006  
1007  
1008  
1009  
1010  
1011  
1012  
1013  
1014  
1015  
1016  
1017  
1018  
1019  
1020  
1021  
1022  
1023  
1024  
1025